2017-03-01

Binder-Jet Printing of Fine Stainless Steel Powder With Varied Final Density

Mohsen Ziaee
University of South Florida, Tampa

Eric M. Tridas
University of South Florida, Tampa

Nathan B. Crane
Brigham Young University - Provo, nbcrane@byu.edu

Binder-Jet Printing of Fine Stainless Steel Powder With Varied Final Density

Mohsen Ziaee[1], Eric. M. Tridas[2], and Nathan B Crane[3]

Keywords: Binder Jetting, stainless steel, Sintering, Porous Materials, Tailored Density

Abstract

Binder jetting is an additive manufacturing process that produces relatively weak porous parts that are strengthened through sintering and/or infiltration. This paper reports on two different methods of preparing fine 316 stainless steel powder and their impact on the final sintered density and dimensions relative to direct printing into -22 micron powder. The first method uses agglomerates of fine powder. In the second, nylon 12 powders are mixed with the steel powder as a fugitive space holder to increase porosity. Sintered density and sintering shrinkage of agglomerate material are shown to vary with the density of the spread powder bed. However, with added nylon the shrinkage correlates with the shrinkage of the base steel powder while the density depends on the quantity of the nylon. Thus, it is possible to create varied sintered density with compatible shrinkage levels—a key step towards creating binder-jetting systems with spatially controlled porosity.

1. Introduction

Additive manufacturing (AM) is a powerful manufacturing method that synthesizes 3D objects in layers directly from a digital definition [1]. Unlike powder bed fusion processes-that employ energy source to fuse the particles-, binder jetting (BJ) utilizes inkjet printing technologies to bond the particles layer by layer. Therefore it can work with a wide range of powdered materials including metals and ceramics. However, the density after printing is about 50% - 60% of the theoretical density and further processing is required to achieve desired properties [2].

Since most BJ work has focused on achieving full density parts, the control of porosity and density in BJ processes has not been extensively explored. The ability of fabricating porous parts with complicated geometries could have broad applications in energy management, lightweight structures, etc. [3]. To approach this goal, this paper addresses direct printing of cured metal

1. Corresponding author: *Email:* mziaee@mail.usf.edu, Department of Mechanical Engineering, University of South Florida, Tampa, FL 33620, Tampa, USA
2, 3. Department of Mechanical Engineerring, University of South Florida, University of South Florida, Tampa, FL 33620, USA

powder and nylon/316L stainless steel mixtures and compares the density and the dimensional variation of the fabricated parts during each stage of the processing. By using metal powders, the total system shrinkage should be reduced compared to printing of oxide powders. A second set of specimens were produced from a mixture of stainless steel powder and a fugitive powder that decomposes during sintering to leave pores. The resulting density and shrinkage are compared to the fine stainless steel powder with and without agglomerates.

2. Experimental

All powder preparations began with raw 316L stainless steel powder with D90<22 μm size obtained from Carpenter Powder Products. Blocks of bound powder were made by tapping the base powder until no further volume change was observed. ExOne M-Flex solvent-based binder was added to the powder at a volume equal to that of 90% of the void volume of the powder. Afterwards, a heating process was performed separately for the powder/binder mixtures at 100°C or 185°C for 4 hours to permit different levels of rearrangement after printing. The lower temperature cured particles are expected to dissolve more fully during printing to permit reorientation. In both cases, the result was a puck of brittle, bound powder. Using a mortar and pestle, the puck was ground to a size of approximately 1–2 mm. These granules were placed into a ball mill with equal volume ¼" 316L stainless steel ball bearings and ground for 30 minute intervals. After each interval, the agglomerate powder was fractioned using a series of sieves and the cured size from 25 to 45 μm were collected to be used in this study.

SEM image of the agglomerates (Figure 1) shows that the agglomerates are irregular in shape with a significant volume of the constituent particles below 10 μm. After preparation, all materials were stored at room temperature in sealed containers in order to reduce moisture absorption. The low temperature cured materials seemed particularly sensitive to moisture absorption and stored with desiccant in the container. If stored without a moisture absorber, the powder would quickly begin to clump together.

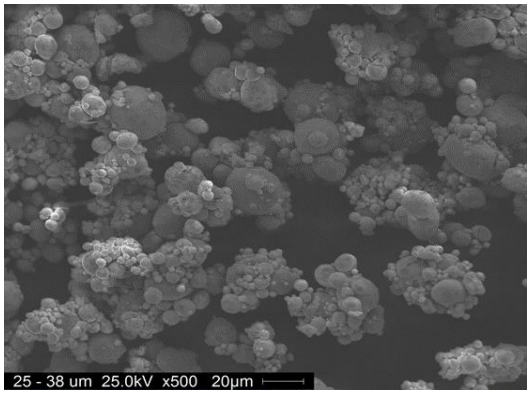

Figure 1. Powder agglomerates cured at 100°C produced using the procedure above; at 25μm-38μm

In the second approach to create porosity, two volume ratios-25% and 33%- of EOS polyamide 12 powder with an average particle size of 55 μm were introduced as a fugitive material

to raw 316L powder. Each batch was prepared by measuring the components and mixing until a visibly homogeneous mixture was produced.

In this study all printing was completed using an ExOne Innovent printing system. The mixed and cured powders were placed on the edge of the print bed where the parts were located. The binder is selectively deposited on the powder bed in layer by layer fashion and the **p**arts are printed on the build platform which travels in the Z-direction. The print head scans along the Y-direction and the linear array of jets that deposit binder are parallel to the X-direction. After printing, the samples were placed in a curing oven for 4 hours at 185°C. The nylon mixes were cured at 140°C to avoid bonding of the unprinted powder due to melting/sintering of the nylon. All dimensional changes were calculated relative to the nominal dimensions of the STL file (5 mm).

Sintering of the green parts was performed under a reducing environment using an Argon/Hydrogen mixture (95% Ar, 5% H_2), which was flowed at a rate of 10 SCFH. Samples were packed into a graphite crucible and supported using a coarse grain alumina powder. Heating rates were *** C/min with a *** min hold at 800°C to assure complete binder and Nylon decomposition. The samples were held at **** C for *** minutes [4].

The bulk, tapped and spread density of each feedstock were quantified with three repetitions of each measurement. The tapped volume of the powders the cylinder was measured in accordance with ASTM B527-15 [5]. To measure the spread densities of the tested powders an 80 μm thick plastic sheet was placed on the build platform. Twenty-four layers of powder of 100 μm thickness each were spread on top of this sheet. A sharp-edged steel punch tool was inserted into the spread bed until it contacted the plastic sheet. The remaining powder around the tool was brushed away and the mass of the powder inside the tool was measured. The sintered density for each part was measured using Archimedes method.

Because of the interparticle forces and humidity, fine powders tend to clump together and corresponds to poor layer spreading characteristics. This issue was more severe as for 316L<22 μm. To approach this problem the powder was sieved and heated up to 50°C for 4 hours to reduce the moisture content before printing.

The key printing parameters are the layer thickness, printing saturation level, and drying conditions. Printing saturation level is defined as the percentage of the powder void space that is filled with printed binder. Typical saturation level are around 60%. Since saturation levels are a function of the spread layer density, an alternative printing parameter termed “binder level” is defined that is powder bed independent. The binder level (β) is defined as the fraction of the part volume that was filled with powder and is related to the saturation (S) by

$$\beta = S(1 - f) \quad (1)$$

where f is the powder bed packing fraction.

As the size and spread density of the powders were different, some adjustments were required in the print parameters. For 316L<22 μm and nylon/316L mixtures the same values were

set on ExOne machine to fabricate the samples because both have fine <10 μm powder particles. However, for the agglomerated powders additional binder was desired to test whether agglomerates binding would dissolve and the particles rearrange. To achieve this, the machine layer thickness was set to 50 μm but deposition of powder was performed every other layer to maintain the same layer thickness but double the printing. The resulting binder loading would be equivalent to printing 100 μm layer at 120% but in two steps with a drying cycle between. To compensate for the higher binder loading, the drying time was also increased to avoid oversaturation and bleeding. Table 1 summarizes the parameters used to fabricate the test samples.

Table I. Summary of key printing parameters used for each powder on ExOne Innovent printer.

	Binder Level	Drying Time (S)	Layer Thickness Setting (μm)
316L<22 μm	24 %	12	100
25% Nylon+316L			
33% Nylon+316L			
Agglomerates(Cured at 100°C)	48 %	20	50
Agglomerates(Cured at 185°C)			

3. Results and discussions

The density measurements (Figure2) demonstrate signficiant variation with powder feed stocks. In all cases, the measured bed density exceeded the density of tapped powder suggesting that the roller was able to re-arrange the particles due to the small thin layers or due to fracturing of the agglomerates, consequently led to the higher bed density. Among the tested samples 316L<22 μm reached the highest packing after layer deposition (56.5 %).

The agglomerated powder shows lower densities when cured at 100°C. It is possible that the moisture form additional bonds to create very irregular powder particles with high level of friction that reduces the compaction quantity. This is consistent with the observation that this powder readily clumped together and did not flow easily. The binding of the low-temperature cured agglomerates should dissolve when wet by fresh binder-permitting particle rearrangements but the lower density does not indicate signficant densification due to rearrangement. In contrast, if the binder is cured at 185°C it will not tend to re-dissolve when exposed to fresh binder—locking the agglomerate powders in place, but these powder agglomerates were more flowable and generated higher density parts.

The agglomerates cured at 185°C showed lower bulk and tapped density than the raw powder, but the spread density is comparable to the untreated powder. It is unusual that the spreading would achieve significantly higher densities than the tapped density. It is possible that the roller is fracturing the agglomerates so that it behaves more like the untreated powder, but when the unused agglomerates were sieved after printing, less than 10% powder was less than 25 μm.

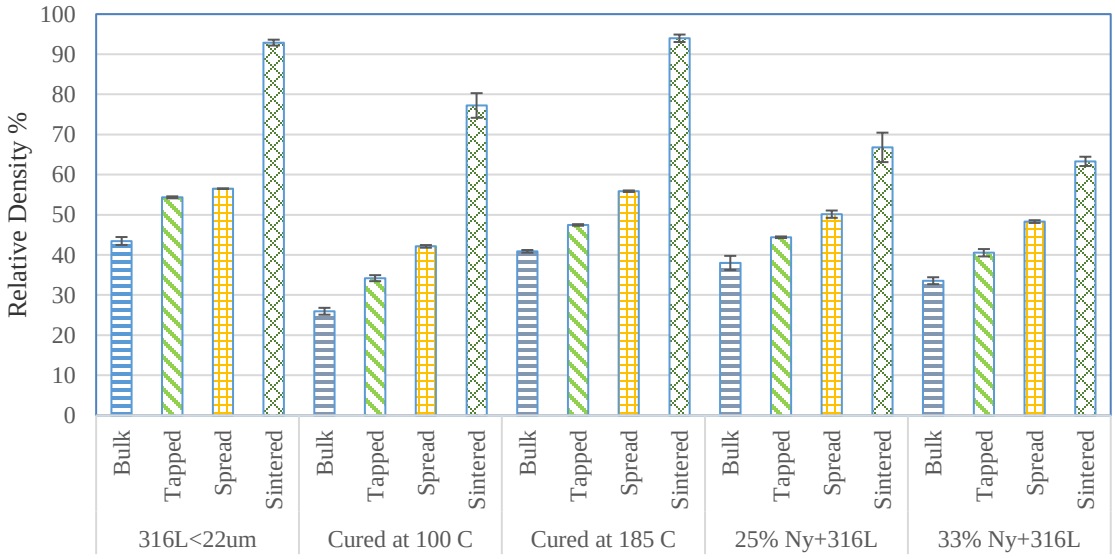

Figure 2. Relative bulk, tapped and spread density for the raw 316 and processed powders. To determine relative density percentage each of the obtained densities was divided over true density of 316L, 7.99 g/cm^3. Error bars represent one standard deviation of the measurements.

The packing density gives evidence of the fundamental occurrences during sintering. It is noticeable that for the tested materials with no nylon addition, the spread density strongly influences the final sintered density. Thus samples with similar spread density (-22 µm raw powder and the agglomerates cured at 185°C) have very similar sintered densities (with 92.9% and 93.9% respectively) whereas this number is 77 % for the agglomerates treated at 100°C.

The nylon mixtures produce a very different response. The mixture spreads to a high packing density. Yet, during sintering, the nylon will decompose leaving voids. These voids are much larger than the voids between steel particles so that they are unlikely to densify through sintering. The results indicate that the final density is not very sensitive to nylon concentration over the range studied with final sintered densities of 66.8% and 63.3% for the powder mixtures with 25% and 33% nylon respectively. The resulting parts have sufficient porosity to be useful for filter, heat exchanger, and other energy applications, but still exhibit good strength. It may be difficult to achieve substantially higher porosities (relative density <40%) by adding a fugitive space filler alone as the remaining structure may not have sufficient strength before and during sintering to maintain the geometry.

The size of the printed parts was measured for each set of conditions and compared to the STL file dimensions (5 mm×5 mm×5 mm). For the agglomerates cured at 100°C the Z-part shrinkage was anomalously large due to a printing error in which several layers were not printed. Figure 3 summarizes the dimensional change after the 1360°C sintering treatment. It can be seen that all samples experienced significant shrinkage in all three axes. It is also noteworthy that the dimensional change in Z direction is highest in every powder type. This suggests that there may be more porosity between layers than within layers.

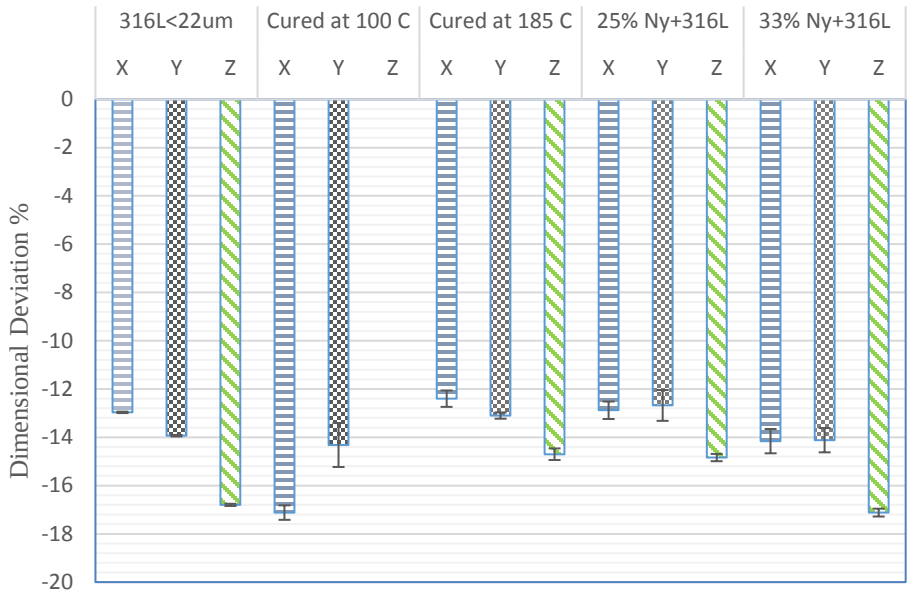

Figure 3. Dimensional deviation for X,Y and Z directions for the sintered samples. Error bars represent one standard deviation of the measured values.

The lowest shrinkage is obtained using the samples with highest spread density except when the fugitive nylon powder is added. The 25% nylon mixture and 185°C cured agglomerates are very closely matched in shrinkage in all three axes despite very different final sintered density (66.8% vs 93.9%). The shrinkage values of these materials may also be compatible with the untreated powder in the X-Y dimensions. Similarly, the as-received <22 μm powder has very similar shrinkage in Y and Z axes to the 33% nylon mixture but with final sintered density of 92.9% and 63.2% respectively.

From the microstructure images shown in Figure 4, it can be seen that most of the pores are attached to the grain boundaries suggesting that grain boundary diffusion is the main bulk transport mechanism driving part densification during sintering [6]. The images also reveal that the samples made with raw 316L powder show small isolated pores formed during the intermediate stage of sintering while for the agglomerates the number of pores declines and the size of the pores become significantly larger.

The nylon mixes show much larger, clearly interconnected porosity. No clear spatial orientation of the pores can be seen. It appears as though the steel regions have densified almost completely (>90%) while the remaining pores arising from the fugitive nylon powder. Because the steel powder is the same in all the samples, the steel sintering should be unchanged—explaining the similar shrinkage levels observed (Figure 3) despite very different final densities.

Most variables that change the final density also change the shrinkage levels. If a part is produced with spatially varying shrinkage levels the part will be distorted during sintering. Since the fugitive nylon mixtures achieve different final densities but with similar processing shrinkage, this process could enable a printing process that can vary density spatially. Such variation could be used to create enhanced heat transfer surfaces if exposed to air or other exchange medium. Alternatively, they could be used internally to reduce heat transfer in undesirable directions. This approach is promising for porosity variation between printed layers. However, it would be difficult to vary the concentration of pore generating particles within the printing plane using most printing processes.

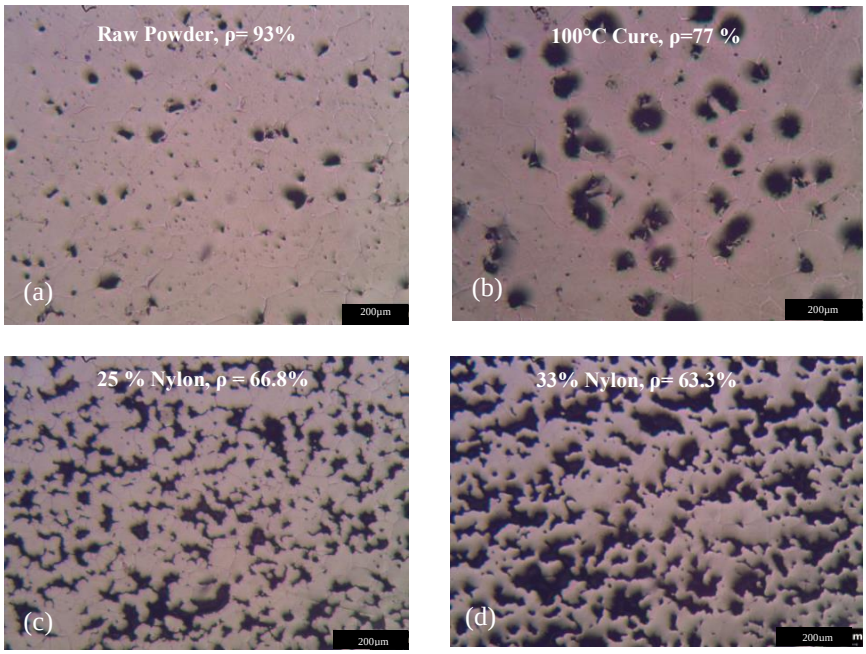

Figure 4. The porosity on the cross-section of the samples made by feedstock materials: a) Raw 316L<22μm b) Agglomerates cured at 100°C c)25% Nylon+316L d) 33% Nylon+316L. Scale bar represents 200 μm.

While new approaches would be needed to get full spatial porosity control, these results suggest a criteria for creating a range of porous structures with similar sintering shrinkage levels. The key criteria is to start with the same base powder, but selectively introduce pores that densify much more slowly than the pores between the finer powder particles. Such a pore structure could be implemented using other mechanisms besides nylon pore generators. If this can be implemented with spatial control, it could be of great use in tuning the properties of printed structures. The resulting voids can also be filled with other materials to introduce new functionalities. Further work is needed to test this hypothesis and to explore the range of porosity values that can be obtained.

4. Conclusion

This paper has assessed the density and shrinkage impact of printing with agglomerates of fine 316 stainless steel and mixtures of steel with nylon powder to results with the base material. These results show that sintered density can be reduced both with agglomerates that spread to a low density and by adding fugitive nylon powders to raw steel powder. Agglomerates that spread well can achieve the same sintered density as the raw powder (>93%). Changes to the sintering process will likely increase the density of both the raw and agglomerate powder closer to full density.

These results also show that fugitive agents can be used to reduce the sintered density below 70% while maintaining compatible shrinkage with high density (>90%) materials. If the shrinkage is the same for different porosity levels, then varied porosity can be created in a single part without deformation due to differential shrinkage rates. This could provide a way to spatially vary critical material properties such as stiffness and thermal conductivity at smaller scales than can be achieved with printed features.

References

[1]. J. Yoo, M. Cima, E. Sachs, and S. Suresh, "Fabrication and Microstructural Control of Advanced Ceramic Components by Three Dimensional Printing," in *Proceedings of the 19th Annual Conference on Composites, Advanced Ceramics, Materials, and Structures—B: Ceramic Engineering and Science Proceedings*, ed: John Wiley & Sons, Inc., 2008, pp. 755-762.
[2]. A. Mostafaei, E. L. Stevens, E. T. Hughes, S. D. Biery, C. Hilla, and M. Chmielus, "Powder bed binder jet printed alloy 625: Densification, microstructure and mechanical properties," *Materials & Design*, vol. 108, pp. 126-135, 10/15/ 2016.
[3]. P. S. Liu and G. F. Chen, "Chapter Three - Application of Porous Metals," in *Porous Materials*, ed Boston: Butterworth-Heinemann, 2014, pp. 113-188.
[4]. J. Song, J. C. Gelin, T. Barrière, and B. Liu, "Experiments and numerical modelling of solid state sintering for 316L stainless steel components," *Journal of Materials Processing Technology*, vol. 177, pp. 352-355, 7/3/ 2006.
[5]. ASTM, "Standard test method for determination of tap density of metallic powders and compounds," ed: ASTM, 2000.
[6]. C. H. Ji, N. H. Loh, K. A. Khor, and S. B. Tor, "Sintering study of 316L stainless steel metal injection molding parts using Taguchi method: final density," *Materials Science and Engineering: A*, vol. 311, pp. 74-82, 7/31/ 2001.